

Thermopower of a Chaotic Quantum Dot

S. F. Godijn, S. Möller, H. Buhmann, and L. W. Molenkamp

II. Physikalisches Institut, RWTH-Aachen, Templergraben 55, D-52056 Aachen, Germany

S. A. van Langen*

Instituut-Lorentz, Leiden University, P.O. Box 9506, 2300 RA Leiden, The Netherlands

(Received 10 November 1998)

The thermovoltage of a chaotic quantum dot is measured using a current heating technique. The fluctuations in the thermopower as a function of magnetic field and dot shape display a non-Gaussian distribution, in agreement with simulations using random matrix theory. We observe no contributions from weak localization or short trajectories in the thermopower. [S0031-9007(99)08804-3]

PACS numbers: 73.20.Dx, 05.45.-a, 72.20.Pa

The electrical conductance of small—characteristic size much smaller than the electron mean free path—confined electron systems (usually denoted as quantum dots) shows distinct fluctuations. These fluctuations display correlations as a function of an external parameter such as shape or magnetic field, which can be described in a statistical manner. The electrons can, in fact, be viewed as billiard balls moving in a classically chaotic system where many random reflections at the system walls occur. Because of the wave-like nature of the electrons, quantum mechanics is needed to describe these systems fully. Chaos in quantum dots has been investigated [1–3] in conductance measurements but the analysis turns out to be difficult. So-called short trajectories [4] and weak localization effects [1,5] add up to the signature of chaotic motion. Moreover, current heating of the electrons in the dot appears to be unavoidable in conductance measurements. Electron heating effects in the dot smear out the underlying chaotic statistics and therefore the observed fluctuations exhibit mostly a Gaussian distribution, although theory predicts non-Gaussian distributions when a small number of electron modes is admitted to the dot [6]. Only when dephasing (modeled as extra modes coupling the dot to the environment) is included, random matrix theory (RMT) [1,7] gives a Gaussian distribution. Very recently, Huibers *et al.* [8] observed small deviations from a Gaussian distribution in conductance measurements. However, other transport properties calculated from these data exhibit again Gaussian distributions, in contrast to theoretical predictions.

An alternative for the conductance measurements pursued so far is to investigate the thermoelectric properties of a system. Thermopower measurements have already been used to study semiconductor nanostructures such as quantum point contacts (QPC) [9] and quantum dots (QD) in the Coulomb blockade regime [10,11]. The thermopower S measures directly the parametric derivative of the conductance, $S \propto G^{-1} \partial G / \partial X$, where $X = E$ (energy), and thus yields both similar and additional information on the electron transport processes as can be obtained from conductance measurements. The distribu-

tion of parametric derivatives ($X = E, B, \text{shape}, \dots$) of the conductance of a QD is the subject of recent RMT investigations [12,13]. The probability distribution for the thermopower is again expected to be non-Gaussian for chaotic conductors, exhibiting cusps at zero amplitude and nonexponential tails [13,14].

In this paper, we present magnetothermopower measurements of a statistical ensemble of chaotic QDs. The observed thermopower fluctuations show a non-Gaussian distribution. We present a numerical fit based on RMT which describes the experimental data. We demonstrate that effects such as short trajectories, weak localization, and dephasing are absent in thermopower measurements.

In Fig. 1a the measured device is shown schematically. A QD (lithographic size $800 \text{ nm} \times 700 \text{ nm}$) is electrostatically defined (gates A, B, C, and D) in a standard, high-mobility 2-dimensional electron gas (2DEG) in a GaAs-(Al,Ga)As heterostructure. The 2DEG has a mobility of $\mu \approx 10^6 \text{ cm}^2(\text{Vs})^{-1}$ for an electron density of $3.4 \times 10^{11} \text{ cm}^{-2}$ at 4.2 K. A $2 \mu\text{m}$ wide and a $20 \mu\text{m}$ long electron-heating channel is defined next to the QD (gates A, D, E, and F). The sample is kept at 40 mK in a dilution refrigerator equipped with a superconducting magnet. Transport measurements are performed using standard phase-sensitive techniques. For reasons of comparison, all data shown in this paper were obtained from the same sample. We have obtained similar results in several other devices.

Conductance data are shown in Fig. 1b. The graph is the magnetoresistance of the QD, averaged over a large number of different configurations [15]. Both QPCs leading to the QD were adjusted to a conductance $G = 4e^2/h$ corresponding to two spin-degenerate modes in the QPCs. As in Ref. [3], an ensemble of configurations was created by repeatedly changing the voltage on gate B by a small amount ($\delta V_g^B = 10 \text{ mV}$). As is evident from the figure, apart from remaining chaotic conductance fluctuations also the signatures of weak localization (sharp peak around $B = 0 \text{ T}$) and short trajectories (characterized by a background conductance that exhibits a polynomial

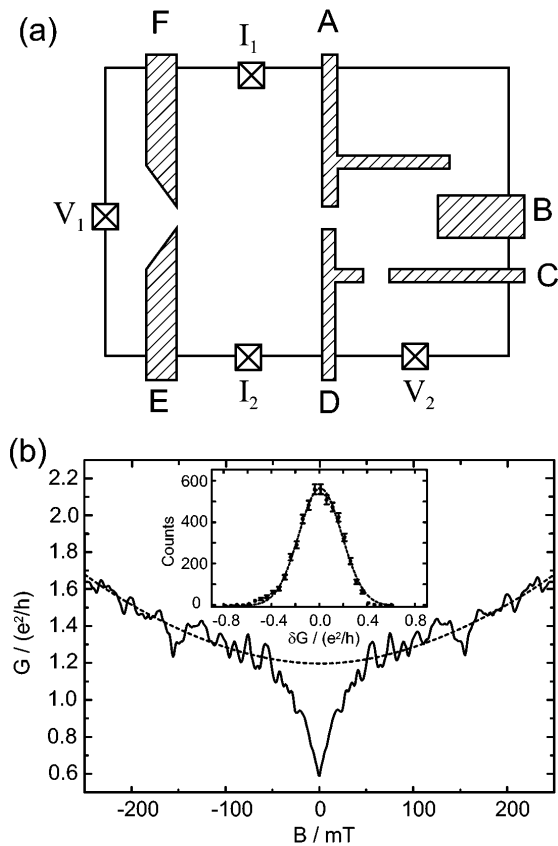


FIG. 1. (a) Schematic top view of the measured sample. The crosses denote the Ohmic contacts to the 2DEG; the hatched areas denote the gates. The heating current is applied between I_1 and I_2 . The thermovoltage is measured between V_1 and V_2 . The QD is defined by applying a negative voltage to gates A, B, C, and D. (b) Magnetoconductance of the QD, averaged over a large number of different QD configurations. The influence of short trajectories is characterized by the dashed line. Inset: Conductance distribution for $|B| \geq 50$ mT

dependence on magnetic field [2,3], Fig. 1b, dashed line) are clearly observed. In order to extract the statistics of the fluctuations, the conductance measurements were corrected for these features. The resulting distribution is shown in the inset of Fig. 1b (for magnetic fields larger than 50 mT). A Gaussian function fits these data well.

By passing a low-frequency (13 Hz) current through the Ohmic contacts I_1 and I_2 , the electron gas in the channel is heated ($T_e \propto I^2$) while the wide 2DEG regions remain in equilibrium with the lattice. The ac heating current $I \approx 0.4 \mu\text{A}$ is small enough to avoid lattice heating, and we have ensured that we are in the regime of linear response. The temperature difference between heating channel and electron reservoir induces a thermovoltage V_{th} across the chaotic QD. V_{th} can be measured, using QPC E-F as a reference point, between Ohmic contacts V_1 and V_2 . V_{th} is then related to the thermopower of the QD, S_{dot} , as

$$V_{\text{th}} = V_2 - V_1 = V_{\text{dot}} - V_{\text{ref}} = (S_{\text{dot}} - S_{\text{ref}})\Delta T. \quad (1)$$

Here, QPC E-F is adjusted such that its thermopower, S_{ref} , is minimal and constant for all measurements. As in the conductance measurements, the transmittance of QPCs A-D and C-D was adjusted to $G = 4e^2/h$. Again, varying the voltage applied to gate B, V_g^B , was used to change the shape of the QD.

In Fig. 2a a gray scale plot is shown of the transverse voltage V_{th} as a function of magnetic field and V_g^B . The step in gate voltage between two successive magnetic-field sweeps was $\delta V_g^B = 10$ mV. The magnetic field range was limited to $|B| \leq 150$ mT to avoid the regime where the quantum Hall effect becomes dominant. The characteristic fluctuations are stable in time and well reproducible. As an example, the trace for $V_g^B = -550$ mV is plotted separately in Fig. 2b. The fluctuations are symmetric around $B = 0$ T with a zero mean.

Because the resistance of the electron heating channel is magnetic-field dependent due to classical (breakdown of the entrance resistance) and quantum (weak localization

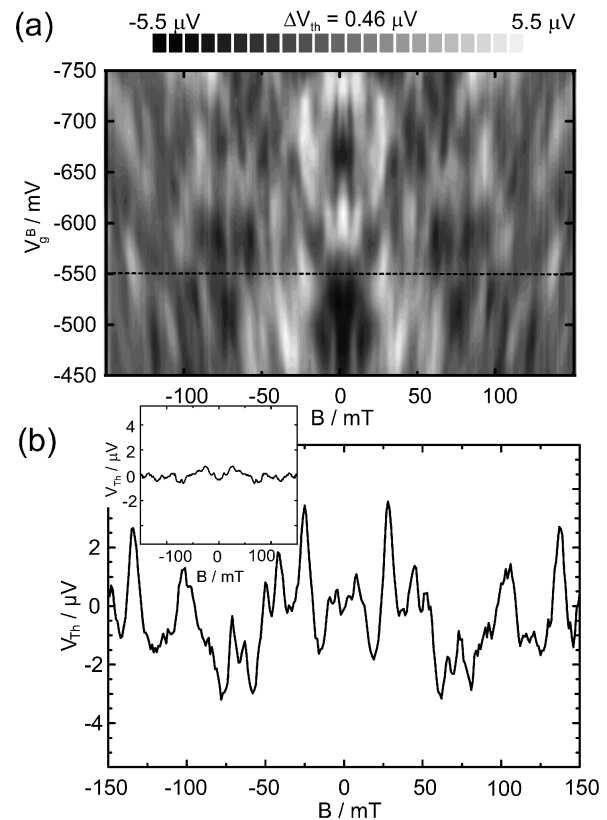


FIG. 2. (a) Gray scale plot of the thermovoltage of the QD as a function of magnetic field (x axis) and of gate voltage on gate B (y axis). The gate voltage is changed by a constant small amount of $\delta V_g^B = 10$ mV for each magnetic field sweep. The light areas denote a large (maximum $5.5 \mu\text{V}$) positive thermovoltage, and the dark areas a large (maximum $-5.5 \mu\text{V}$) negative thermovoltage. (b) Individual thermovoltage trace for $V_g^B = -550$ mV [dashed line (a)]. Inset: Thermovoltage, corrected for the temperature variation of the heating channel and averaged over a large number of QD configurations. Signatures of weak localization and short trajectories are absent.

and conductance fluctuations) transport effects, also the electron temperature in Eq. (1) is somewhat dependent on magnetic field, $T_e = T_e(B)$. For the given device structure, this dependence can easily be determined experimentally, using the quantized thermopower of a QPC [9]. The thermovoltage of QPC A-D, adjusted for maximum thermopower, is measured as a function of magnetic field while keeping $V_g^B = V_g^C = 0$ V, i.e., without defining the QD, yielding $V_{th,channel} = (S_{AD} - S_{ref})\Delta T(B)$. The variation in channel temperature, which turns out to be only a few percent, is effective for each individual measurement. Thus, by dividing the QD thermovoltage by the QPC thermovoltage, this effect can be eliminated. We have verified that this calibration does not influence the statistics of the thermopower fluctuations.

The inset of Fig. 2b shows the temperature-variation corrected thermovoltage, averaged over all configurations. We show this averaged trace to illustrate that in contrast to the averaged conductance (Fig. 1b) signatures of weak localization and short trajectories are absent in the averaged thermopower [15]. For the weak localization correction, this is readily understood when one realizes that the correction to the conductance for a zero-dimensional system is energy independent, and any signs of weak localization in the thermopower should derive from the energy dependence of the phase-coherence length l_ϕ which is presumably small. (However, see Ref. [16] for experiments on weak localization thermopower in the two-dimensional quantum-diffusive transport regime.) The absence of a signature of short trajectory effects in the thermovoltage measurements implies also a very weak energy dependence for the conductance correction due to these processes. Heuristically, one might argue that the fast transit times involved with short trajectories correspond to large energy scales while the thermopower measures a local (at E_F) derivative. It would be interesting to investigate these effects theoretically.

We now proceed to compare the statistics of the observed thermopower fluctuations with theoretical predictions. The system symmetry, denoted in RMT with an integer β , changes with magnetic field; around $B = 0$ T, time-reversal symmetry (TRS, $\beta = 1$) is present, while for higher magnetic fields this symmetry is broken ($\beta = 2$). The transition between the two regimes is gradual; for the present analysis we restrict ourselves to the two extremes. Experimentally, the regime with TRS is the magnetic-field range where the weak localization effect dominates conductance measurements ($|B| \leq 40$ mT); TRS is broken for $|B| \geq 50$ mT. Counting the fluctuation amplitudes of the corrected thermopower for these two regimes leads to the histograms presented in Fig. 3. The dashed lines are the best Gaussian fit to the experimental data. Clearly, strong deviations from Gaussian statistics occur.

These deviations are also expected from RMT calculation. In Ref. [14], the thermopower distribution of a chaotic QD has been obtained for single-mode con-

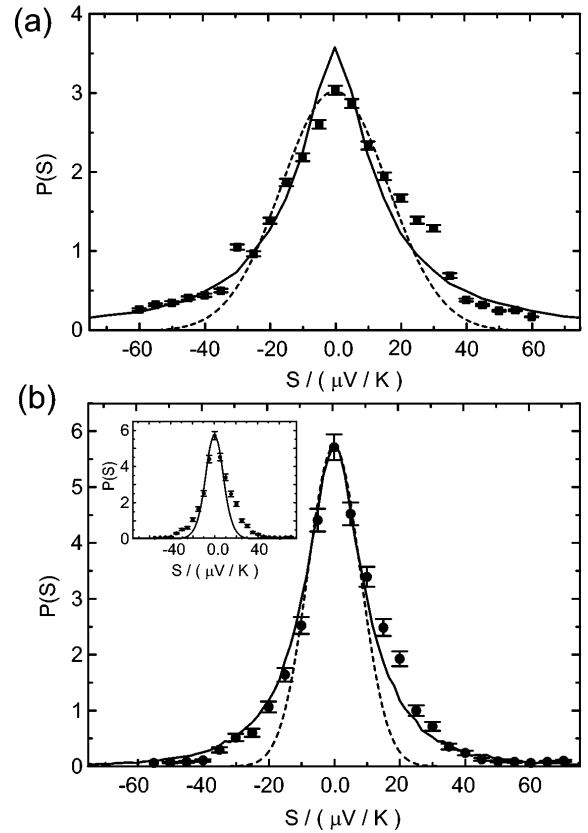


FIG. 3. (a) Thermopower distribution in the presence of TRS ($|B| \leq 40$ mT). Experimental results (dots), simulation results (solid line), and Gaussian fit (dashed line). (b) Thermopower distribution for broken TRS ($|B| \geq 50$ mT). Experimental results (dots), simulation results (solid line), and Gaussian fit (dashed line). Inset: Experimental thermopower distribution (dots) for broken TRS, compared to simulation results including strong dephasing (solid line).

tacts. The distribution exhibits a cusp at $S = 0$ and tails as $P(S) \propto |S|^{-1-\beta} \ln |S|$, which displays a clear deviation from a Gaussian distribution. However, for a large number of conducting channels this distribution becomes again Gaussian. For the experimental data, taken with two spin-degenerate conducting modes in the leads, deviations from the Gaussian distribution are still expected. Since in RMT an analytical treatment for the thermopower distribution is possible only for single-mode leads, Monte Carlo simulations have to be employed for the present system. The Hamiltonian \mathcal{H} of the closed QD is drawn randomly from the Gaussian ensemble

$$P(\mathcal{H}) \propto e^{-c\text{Tr}\mathcal{H}\mathcal{H}^\dagger}, \quad (2)$$

where c is a constant setting the mean level spacing Δ and \mathcal{H} is real symmetric ($\beta = 1$) or Hermitian ($\beta = 2$). The scattering matrix M of the open system is calculated from \mathcal{H} using [17]

$$M(E) = 1 - 2\pi i W^\dagger (E - \mathcal{H} + i\pi W W^\dagger)^{-1} W. \quad (3)$$

Here, W is a rectangular matrix coupling the states in the QD to the scattering channels. The thermopower is then calculated from

$$S = -\frac{\pi^2}{3} \frac{k_B^2 T}{e} \frac{d}{dE} \ln T(E) \Big|_{E=E_F}, \quad (4)$$

where $T(E) = \sum_{\alpha \in 1, \beta \in 2} |M_{\alpha\beta}|^2$ is the probability for the transmission from lead 1 to lead 2. The differentiation is done numerically for each realization of the Hamiltonian. The density of states $\rho(E_F) = 1/2\pi i \text{Tr}(M^\dagger dM/dE)|_{E=E_F}$ is used as a weight factor to account for a large charging energy [13]. The resulting distributions of the thermopower fluctuations for both symmetry classes are shown as solid lines in Fig. 3. Evidently, the simulations represent the experimental results much better than a Gaussian distribution function.

For a comparison of experimental and theoretical distributions, the horizontal axes of both data sets have to be scaled, while keeping the normalization (area equals one). Only one scaling parameter was needed to fit the distributions for TRS and broken TRS (Fig. 3), which implies a temperature difference across the QD of $\Delta T = 56$ mK. As an independent check for the correctness of this scaling procedure, we have in addition measured the thermovoltage (for the same heating current) across QPC A-D, adjusted for maximum thermovoltage, i.e., between the $N = 1$ and $N = 2$ conductance plateaus [9]. For this configuration, the thermopower of a QPC is quantized, directly yielding a value for ΔT . We find $\Delta T = 54$ mK at $I = 0.4 \mu\text{A}$, in good agreement with the scaling result.

It is possible to show that in thermopower measurements dephasing corrections, which are used to explain Gaussian conductance fluctuation distributions of chaotic QDs, are indeed irrelevant. The influence of a finite phase-coherence time τ_ϕ can be studied by connecting the QD to a third virtual reservoir. The bath is coupled via $N_\phi \gg 1$ channels, corresponding to the incoherent limit ($\hbar/\tau_\phi \gg \Delta$). The chemical potential μ_ϕ and temperature T_ϕ of the bath are chosen exactly in between those of the real reservoirs, such that it draws neither charge nor heat current. The distribution of the thermopower for broken TRS ($\beta = 2$) is then given by

$$P(\sigma) = 2^{-8N^2+1} N e^{-N|\sigma|} \times \sum_{k=0}^{4N^2-1} \binom{8N^2-2-k}{4N^2-1} \frac{1}{k!} |2N\sigma|^k, \quad (5)$$

$$\sigma = \frac{3e}{\pi k_B^2 T \Delta} \left(\frac{\hbar}{\tau_\phi} \right)^2 S.$$

The result of Eq. (5) is plotted for $N = 2$ in the inset of Fig. 3b (solid line). It can be seen that there is only little agreement between the experimental thermopower data and theory including dephasing which proves that

the observed statistics do not indicate the presence of any dephasing induced by electron heating.

In conclusion, we have demonstrated that the thermopower measurements on a chaotic QD reveal directly the theoretically predicted non-Gaussian fluctuation distributions. In contrast to the best results obtained so far in conductance measurements, we do not have to include thermal broadening or dephasing to model our experimental results. Another distinction from conductance measurements is that the thermopower data are not influenced by weak localization or short trajectories. Therefore, thermopower measurements can be considered as an excellent tool in the area of investigating chaotic quantum transport properties in open systems.

We thank C.W.J. Beenakker for his interest in this work. Part of this work was supported by the DFG, SFB-341 and DFG MO 771/3.

*Present and permanent address: Philips Research Laboratories, 5656 AA Eindhoven, The Netherlands.

- [1] C. W. J. Beenakker, *Rev. Mod. Phys.* **69**, 731 (1997).
- [2] C. M. Marcus *et al.*, *Phys. Rev. Lett.* **69**, 506 (1992).
- [3] I. H. Chan *et al.*, *Phys. Rev. Lett.* **74**, 3876 (1995).
- [4] H. U. Baranger and P. A. Mello, *Europhys. Lett.* **33**, 465 (1996).
- [5] Z. Pluhar, H. A. Weidenmüller, J. A. Zuk, and C. H. Lewenkopf, *Phys. Rev. Lett.* **73**, 2115 (1994); H. U. Baranger, R. A. Jalabert, and A. D. Stone, *Phys. Rev. Lett.* **70**, 3876 (1993).
- [6] K. B. Efetov, *Phys. Rev. Lett.* **74**, 2299 (1995).
- [7] H. U. Baranger and P. A. Mello, *Phys. Rev. B* **51**, 4703 (1995); P. W. Brouwer and C. W. J. Beenakker, *Phys. Rev. B* **51**, 7739 (1995); P. W. Brouwer and C. W. J. Beenakker, *Phys. Rev. B* **55**, 4695 (1997).
- [8] A. G. Huibers *et al.*, *Phys. Rev. Lett.* **81**, 1917 (1998).
- [9] L. W. Molenkamp, H. van Houten, C. W. J. Beenakker, R. Eppenga, and C. T. Foxon, *Phys. Rev. Lett.* **65**, 1052 (1990).
- [10] L. W. Molenkamp *et al.*, *Semicond. Sci. Technol.* **9**, 903 (1994); A. A. M. Staring *et al.*, *Europhys. Lett.* **22**, 57 (1993).
- [11] S. Möller, H. Buhmann, S. F. Godijn, and L. W. Molenkamp, *Phys. Rev. Lett.* **81**, 5197 (1998).
- [12] Y. V. Fyodorov, *Phys. Rev. Lett.* **73**, 2688 (1994); Y. V. Fyodorov and A. D. Mirlin, *Phys. Rev. B* **51**, 13403 (1995).
- [13] P. W. Brouwer *et al.*, *Phys. Rev. Lett.* **79**, 913 (1997).
- [14] S. A. van Langen, P. G. Silvestrov, and C. W. J. Beenakker, *Superlattices Microstruct.* **23**, 691 (1998).
- [15] Small fluctuations are still visible both in the averaged conductance (Fig. 1b) and the averaged thermovoltage (inset of Fig. 2b) due to the limited range of gate voltage V_g^B that is accessible in the experiment without destroying the sample.
- [16] M. J. Kearney, R. T. Stone, and M. Pepper, *Phys. Rev. Lett.* **66**, 1622 (1991).
- [17] J. J. M. Verbaarschot, H. A. Weidenmüller, and M. R. Zirnbauer, *Phys. Rep.* **129**, 367 (1985).